

DYNAMIC MODEL OF ARTIFICIAL REACTIVE IMPEDANCE SURFACES

S. A. Tretyakov

Radio Laboratory
Helsinki University of Technology
Finland

C. R. Simovski

Physics Department
St. Petersburg Institute for Fine Mechanics and Optics
Russia

Abstract—New artificial reactive impedance surfaces have been recently suggested by Sievenpiper et al. for antenna and waveguide applications. In particular, high impedance values corresponding to a magnetic wall can be realized in dense arrays of conducting patches over a conducting plane. In this paper, a dynamic model for the electromagnetic properties of such structures is developed. The analytical model takes into account electromagnetic interactions between all patches in infinite arrays excited by normally incident plane waves, as well as higher-order Floquet modes between the array and the ground plane. The results are compared with the known experiments.

1 Introduction

2 Equivalent Surface Impedance

2.1 Grid Impedance

2.2 Equivalent Surface Impedance and Reflection Coefficient

2.3 Equivalent Circuit Parameters

3 Generalizations

3.1 Sparse Arrays

3.2 Higher-Order Modes Influence

3.3 Influence of the Dielectric Layer on the Grid Impedance: Dynamic Correction

4 Comparison with the Local Quasi-Static Model and Experiment

5 Conclusion

Acknowledgment

References

1. INTRODUCTION

Recently, new artificial impedance surfaces were suggested and investigated in several papers [1–7]. They are basically periodical structures of densely packed planar conducting patches or complimentary arrays of slots in metal planes. For arrays of patches positioned in close proximity to a solid metal plane as in [1, 2], periodically positioned vias wires are introduced to prevent electromagnetic waves from traveling in the waveguide between the array and the ground. Because of the specific geometry, this structure is sometimes named *mushroom* array, see the geometry in Fig. 1. These novel artificial layers are also called 2D photonic (or *electromagnetic*, which is more appropriate for the frequency band of applications) bandgap structures. Suggested applications mainly utilize existing stop bands for waves propagating along these surfaces. Potential applications are in antennas [1, 8] and microwave filters [7].

In modeling both 2D and 3D structures, local quasi-static models have been previously used [1, 7]. In the simple local model of mushroom layers introduced by Sievenpiper et al., the structure was essentially considered as an array of non-interacting cells, although sharing the same magnetic flux. Each cell was characterized by its quasi-static parameters, capacitance and inductance. The equivalent capacitance was calculated as the capacitance of a single cell, thus, no field interaction between cells through their electric fields was taken into account. The adopted local and quasi-static approximation resulted in an equivalent circuit representation in the form of a parallel circuit. However, it is known that patches in dense arrays strongly interact, and the parameters of arrays can be only roughly estimated from the parameters of individual inclusions. A more accurate model was used in [3] in studies of TM waves along the Sievenpiper mushroom surface. In that study, the space between the patches and the ground was replaced by a transmission line filled by a uniaxial dielectric, and the patch array was modeled by an equivalent capacitive reactance. Numerical solutions for such periodical structures can be easily obtained, for example using the periodical method of moments. For

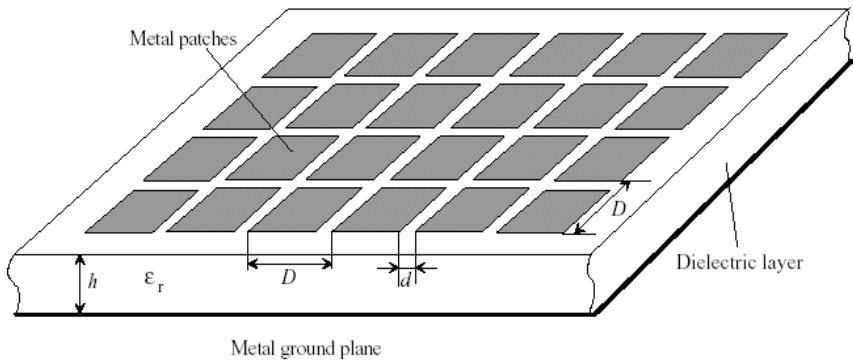


Figure 1. Geometry of the artificial impedance surface. Array of conducting patches is located at distance h from the ground plane. The space between the array and the ground is filled by a dielectric with the relative permittivity ϵ_r .

example in paper [4] arrays of rectangular patches over a metal plane have been analyzed numerically with the goal to eliminate surface wave propagation along the surface.

In this paper we build analytical dynamic model of 3D (mushroom) artificial surfaces, which takes into account electromagnetic interactions of all cells. The geometry can be seen from Figure 1. The present model is valid for small square patches compared to the wavelength (array period $D \ll \lambda$) and narrow slots between patches (slot width $d \ll D$). The distance to the ground is h .

Our goal here is to develop an analytical full-wave model of the equivalent surface impedance. The present theory is restricted to the normal-incidence plane-wave excitation. In particular, this means that vias conductors connecting patches to the ground are not excited, and there is no need to take them into account. So the system we model consists of a periodical planar array of ideally conducting patches positioned parallel to an infinite conducting plane, at a small distance. A dielectric substrate can be positioned between the array and the ground.

2. EQUIVALENT SURFACE IMPEDANCE

Here we will introduce and calculate the equivalent surface impedance of reactive impedance surfaces. We will do it for both capacitive grids near conducting planes (arrays of patches as in Figure 1) and the complimentary structure of inductive grids (arrays of thin conducting strips in place of the gaps between the patches).

2.1. Grid Impedance

Electromagnetic properties of planar grids of this kind can be described in terms of the grid impedance Z_{grid} which connects the averaged electric field in the grid plane and the averaged current density:

$$\langle E \rangle = Z_{\text{grid}} \langle J \rangle \quad (1)$$

Normal plane-wave incidence is assumed here. In case of an inductive grid formed by thin parallel conducting strips, the grid impedance in (1) is [9, 10]:

$$Z_{\text{grid}} = Z_{\text{strips}} = j \frac{\eta}{2} \kappa \quad (2)$$

where

$$\kappa = \frac{kD}{\pi} \log \left(\frac{2D}{\pi d} \right) \quad (3)$$

is the grid parameter, and we use the standard notations for the wave number $k = \omega \sqrt{\epsilon_0 \mu_0}$ and the wave impedance $\eta = \sqrt{\mu_0 / \epsilon_0}$. Relation (3) was originally derived for grids of thin round wires, period $D \ll \lambda$. Here we have replaced the wire radius $r_0 \ll D$ by the equivalent planar strip thickness $d = 4r_0$. The model is suitable for thin conducting strips as compared to the grid period ($d \ll D$). If this is not so, the homogenization model [11] can be used instead. The difference is in the value of parameter κ (a different expression under the logarithm function). Averaging and homogenization procedures leading to (1) take into account electromagnetic interactions in infinite grids. Simplifications are in the cell models: the cell size is assumed to be small compared to the wavelength, so that the local field distribution over a cell is assumed to be close to the quasi-static distribution. This restriction will be lifted in Section 3.1.

For the complimentary array of conducting patches in free space the grid impedance can be found using the Babinet principle (e.g. [15]):

$$Z_{\text{grid}} = Z_{\text{patches}} = \frac{\eta^2}{4Z_{\text{strips}}} \quad (4)$$

In terms of the grid parameter κ this gives

$$Z_{\text{patches}} = -j \frac{\eta}{2\kappa} \quad (5)$$

that is, one can simply replace κ by $-1/\kappa$. If there is a dielectric material on one side of the grid (and there is free space on the other

side), the symmetry which leads to the Babinet principle is missing, and (4) is not valid. However, there is an approximate formula [12]

$$Z_{\text{grid}} = Z_{\text{patches}} = \frac{\eta^2}{4Z_{\text{strips}}} \frac{2}{\epsilon_r + 1} = -j \frac{\eta}{2} \frac{1}{\kappa} \frac{2}{\epsilon_r + 1} \quad (6)$$

where ϵ_r is the relative permittivity of the lower half space. The last formula is very accurate for grids whose period is small compared to the wavelength, which is our main case of interest.

The above theory neglects electric polarization in thin conducting strips ($d \ll D$) when the incident electric field is orthogonal to the strip. An approximate formulation of the Babinet principle which takes into account that effect has been published in [13].

2.2. Equivalent Surface Impedance and Reflection Coefficient

Let us now consider a grid positioned parallel to a conducting plane, and assume first that the distance from the grid to the ground h is not smaller than the grid period D . In this situation we can neglect higher-order Floquet modes generated by the periodical mesh. Assuming only the fundamental-mode plane waves between the array and the ground, the equivalent surface impedance can be easily found as the impedance of a parallel connection of the grid impedance Z_{grid} and the input impedance of a TEM line section of length h ($Z = j\eta_- \tan(k_-h)$, where $k_- = k\sqrt{\epsilon_r}$ and $\eta_- = \eta\sqrt{1/\epsilon_r}$ are the parameters of the medium between the array and the ground plane). The input impedance is found from

$$\frac{1}{Z_{\text{inp}}} = \frac{1}{j\eta_- \tan(k_-h)} + \frac{1}{Z_{\text{grid}}} \quad (7)$$

The normalized equivalent surface impedance we define as

$$Z_s = \frac{Z_{\text{inp}}}{\eta} = \frac{\frac{Z_{\text{grid}}}{\eta} \tan(k_-h)}{\tan(k_-h) - j \frac{Z_{\text{grid}}}{\eta_-}} \quad (8)$$

Interpretation of Z_s singularity at the frequency where the denominator of (8) equals zero as a parallel resonance of the array and the transmission line formed by spacing h between the patches and the ground plane is evident.

In terms of the grid parameter κ we have

$$Z_s = \frac{j \frac{\kappa}{2} \tan(k_-h)}{\tan(k_-h) + \sqrt{\epsilon_r} \frac{\kappa}{2}} \quad (9)$$

for arrays of conducting strips and, using (6),

$$Z_s = \frac{j \frac{1}{\sqrt{\epsilon_r}} \tan(k-h)}{1 - \frac{\epsilon_r+1}{\sqrt{\epsilon_r}} \kappa \tan(k-h)} = \frac{j \frac{1}{\sqrt{\epsilon_r}} \tan(k-h)}{1 - \frac{(\epsilon_r+1)kD}{\pi\sqrt{\epsilon_r}} \log\left(\frac{2D}{\pi d}\right) \tan(k-h)} \quad (10)$$

for arrays of patches. The last simple formula can be used to calculate the equivalent surface impedance of Sievenpiper impedance surfaces for normally incident plane waves. As will be shown in the next section, the result can be extended to resonant grids and corrected to account for higher-order Floquet modes by appropriate modifications of the grid parameter κ .

Replacing $\tan(k-h)$ by its argument for the case of small $k-h$ and multiplying by η (for the surface impedance in Ohm) yields Z_s in the form which coincides with the result from the known parallel circuit model [1]:

$$\eta Z_s = \frac{j\omega L}{1 - \omega^2 LC} \quad (11)$$

where

$$L = \mu_0 h, \quad C = \frac{D\epsilon_0(\epsilon_r + 1)}{\pi} \log\left(\frac{2D}{\pi d}\right) \quad (12)$$

It is important that for realistic and practical sizes the resonant frequency is not very low due to rather small values of the effective capacitance and inductance, and the structure thickness turns out to be not very much smaller than the resonant wavelength. Therefore, the use of formula for the resonant frequency which follows from (11), i.e.,

$$\omega_0 = \frac{1}{\sqrt{LC}} \quad (13)$$

leads to errors of order $(0.1 - 0.2)\omega_0$, so it is preferable to use formula (10).

The reflection coefficient is, obviously,

$$R = \frac{Z_s - 1}{Z_s + 1} \quad (14)$$

If there is no dielectric layer between the array and the ground plane ($\epsilon_r = 1$), the reflection coefficient can be written also as

$$R = -e^{-2jkh} - \frac{(1 - e^{-2jkh})^2}{1 - e^{-2jkh} + j\kappa} \quad (15)$$

2.3. Equivalent Circuit Parameters

Let us compare the low-frequency equivalent parameters (12) with the known quasi-static approximations [2]. The value of inductance L is the same as in [2], but the equivalent capacitance C is different, since it takes into account cell interactions. The local and quasi-static estimation of C from [2, p. 39] is as following:

$$C = \frac{D\epsilon_0(\epsilon_r + 1)}{\pi} \log \left[\left(\frac{2D}{d} \right) + \sqrt{\left(\frac{2D}{d} \right)^2 - 1} \right] \quad (16)$$

$$\approx \frac{D\epsilon_0(\epsilon_r + 1)}{\pi} \log \left(\frac{4D}{d} \right)$$

Note that formula (16) in [2] was derived from the electric flux density per unit length in a gap between two metallic half-planes. Because this capacitance is infinite, the electric field flux was truncated at distance D from the slit to obtain the capacitance per unit length between two coplanar strips of width D . However, the capacitance per unit length of two coplanar strips of width D can be found exactly using the conformal mapping method. For the case $d \ll D$ its expression via the elliptic integrals can be simplified to (the free-space case)

$$C = \frac{4D\epsilon_0}{\pi} \log \frac{4}{\sqrt{1 - k'^2}} \quad (17)$$

where $k' = \frac{1}{1+d/D}$. For very small d/D this reduces to

$$C \approx \frac{2D\epsilon_0}{\pi} \log \frac{8D}{d} \quad (18)$$

Comparing to a more accurate expression (12), we see that the correction can be quite essential, depending on the geometry. It is interesting to note that a less accurate static expression (16) for the cell capacitance eventually leads to estimations which are closer to the result of the dynamic theory which only stresses the shortcoming of the quasi-static model.

3. GENERALIZATIONS

3.1. Sparse Arrays

Restriction $D \ll \lambda$ can be easily lifted for the case when the system is in free space ($\epsilon_r = 1$), since an accurate expression for the grid

parameter κ is available [10]:

$$\kappa = \frac{kD}{\pi} \left[\log \frac{2D}{\pi d} + \frac{1}{2} \sum'_{n=-\infty}^{\infty} \left(\frac{2\pi}{\sqrt{(2\pi n)^2 - k^2 D^2}} - \frac{1}{|n|} \right) \right] \quad (19)$$

(the term with $n = 0$ is excluded from the summation). Substitution of (19) into (10) defines the array equivalent impedance without restriction on the patch size. Note that for $D > \lambda$ the surface impedance has a non-zero real part, which describes diffraction loss due to excitation of grating lobes. For moderate kD one can use the Taylor expansion of the series in (19):

$$\kappa = \frac{kD}{\pi} \left[\log \frac{2D}{\pi d} + \frac{\zeta(3)}{2} \left(\frac{kD}{2\pi} \right)^2 + \frac{3\zeta(5)}{8} \left(\frac{kD}{2\pi} \right)^4 + \dots \right] \quad (20)$$

where $\zeta(x)$ is the Riemann zeta function.

3.2. Higher-Order Modes Influence

It is known that the field scattered by wire and strip meshes excited by plane waves does not practically differ from a plane wave at distances larger than the grid period D . It means that even if h is small compared to the wavelength but large compared to D , one can consider the interaction between the grid and the metal plane as the far-zone one. It leads to the transmission-line formula for the equivalent impedance of the grid parallel to a metal plane, which was used above and in [3]. However, if h becomes smaller than D , one should take into account the influence of higher-order (evanescent) Floquet modes reflected by the ground plane.

Let us again consider a single grid of thin parallel wires or thin strips in free space excited by a normally incident plane wave polarized along the wires. The grid period D is assumed to be small compared to λ , and the diameter of wires (or the width of strips) is small compared to D . The field scattered by the grid does not essentially differ from that of a square mesh since the orthogonal array of thin wires is practically not excited. The scattered field can be calculated exactly (for thin strips) using the Poisson summation rule:

$$\begin{aligned} E_g(y, z) &= -\frac{k\eta}{4} I \sum_{n=-\infty}^{\infty} H_0^{(2)}(k\sqrt{z^2 + (y - nD)^2}) \\ &= -\frac{k\eta}{2} \frac{I}{D} \sum_{m=-\infty}^{\infty} \frac{e^{-j\frac{2\pi y}{D}m - j\sqrt{k^2 - (\frac{2\pi m}{D})^2}|z|}}{\sqrt{k^2 - (\frac{2\pi m}{D})^2}} \end{aligned} \quad (21)$$

Here I is the induced current in strips related with the averaged surface current as $J = \langle J \rangle / D$, z and y are coordinates of the observation point with respect to the reference wire positioned at the origin $y = z = 0$ (axis z is orthogonal to the grid plane). For dense grids ($D \ll \lambda$) one can approximate $\sqrt{k^2 - \left(\frac{2\pi m}{D}\right)^2} \approx -j\frac{2\pi m}{D}$ for $m \neq 0$, then the previous formula simplifies as

$$E_g(y, z) = -\frac{k\eta}{2} \frac{I}{D} \left(\frac{e^{-jk|z|}}{k} + jS(y, z) \right), \quad (22)$$

$$S = \frac{D}{\pi} \operatorname{Re} \left[\sum_{m=1}^{\infty} \frac{e^{-j\frac{2\pi y}{D}m} e^{-\frac{2\pi|z|}{D}m}}{m} \right]$$

The first term in the expression for E_g is the uniform part of the the scattered field (reflected and transmitted plane waves), and the second term proportional to S is its fluctuating part containing all the evanescent modes in closed form [14]:

$$S = -\frac{D}{\pi} \operatorname{Re} \left[\log(1 - e^{-\frac{2\pi}{D}(jy+|z|)}) \right] \quad (23)$$

Next, we consider the same grid of wires at height h over a ground plane. To find the total scattered field we apply the image approach. The influence of the ground plane is represented as the field re-radiated by the image grid plus the image of the incident wave. The total field at the surface of the reference wire is

$$E_{\text{tot}} = \frac{-k\eta}{2D} \left(\frac{e^{-jk|r_0|}}{k} + jS(0, r_0) \right) I \quad (24)$$

$$+ \frac{k\eta}{2D} \left(\frac{e^{-2jkh}}{k} + jS(0, 2h) \right) I + E_{\text{inc}}(1 - e^{-2jkh})$$

where E_{inc} is the incident electric field. Here we have assumed that the wire radius r_0 or the equivalent strip width $d = 4r_0$ is small compared to h , in which case $S(0, r_0) \approx \frac{D}{\pi} \log \frac{D}{2\pi r_0}$. The boundary condition on a conducting wire $E_{\text{tot}} = 0$ allows to find the induced current I . Finally, writing the reflected field as

$$E_{\text{ref}} = -\frac{\eta I}{2D} (1 - e^{-2jkh}) - E_{\text{inc}} e^{-2jkh} \quad (25)$$

we find that formula (15) is replaced by

$$R = -e^{-2jkh} - \frac{(1 - e^{-2jkh})^2}{1 - e^{-2jkh} + j(\kappa + \gamma)} \quad (26)$$

The only influence of the evanescent modes is the substitution $(\kappa + \gamma)$ instead of κ , where

$$\gamma = \frac{kD}{\pi} \log(1 - e^{-\frac{4\pi h}{D}}) < 0 \quad (27)$$

For the case when the inequality $D \ll \lambda$ is not valid, the correction term cannot be calculated in closed form, but an expression via a very quickly convergent series is available [16]:

$$\gamma = \frac{kD}{\pi} \sum_{m=1}^{\infty} \left(\frac{1 - e^{-4\pi \frac{h}{D} \sqrt{m^2 - (\frac{kD}{2\pi})^2}}}{\sqrt{m^2 - (\frac{kD}{2\pi})^2}} - \frac{1}{m} \right) \quad (28)$$

The higher-order modes influence turns out to be negligible even if $h \sim D/2$, and it becomes essential only if the thickness h is small compared to D . In the following, calculating the impedance of arrays of patches through that of the square mesh of strips with Eq. (10) we substitute $\kappa \rightarrow \kappa + \gamma$.

3.3. Influence of the Dielectric Layer on the Grid Impedance: Dynamic Correction

The previous theory has been based on an estimation for the grid impedance of arrays of thin conducting strips (2)–(3). Although that theory takes into account dynamic interaction of the strips in the infinite arrays, the local field distribution near a strip is assumed to be quasi-static[†]. Under this approximation the grid impedance (2) is purely inductive and its value does not depend on the permittivity of the medium in which the grid is located. The grid impedance of the complementary grid of patches (6) is, naturally, a pure capacitance which does not feel the permeability of the medium.

A more accurate theory of artificial impedance layers can be built using a result from [17], where the averaged boundary conditions (AvBC) have been derived for a square mesh of wires positioned at an arbitrary distance (including the case of zero distance) from an interface between two dielectrics. In that work the author applied the exact image method to calculate the field of an infinitely long perfectly conducting wire (or a thin strip) near an interface, and using that result the electromagnetic interaction of currents induced in the mesh wires was studied. The AvBC determine the relation between the electric field averaged over the mesh period and the averaged induced surface

[†] The nature of the approximation can be seen from Section 3.2. Repeating the derivation in the absence of the ground plane one arrives to (3).

current, as in (2). The general result presented in [17] (formula (2.25), page 49) refers to a non-orthogonal mesh and arbitrary wave incidence. For square meshes and normal incidence it reads (in our notations) as:

$$\langle \mathbf{E} \rangle = j \frac{\eta}{2} \kappa_{\text{eff}} \langle \mathbf{J} \rangle, \quad \kappa_{\text{eff}} = \frac{kD}{\pi} (1 - \Delta) \log \frac{2D}{\pi d} = \kappa (1 - \Delta) \quad (29)$$

where the correction term

$$\begin{aligned} \Delta = & \frac{2}{\log \frac{2D}{\pi d}} \int_0^\infty \frac{J_2(p)}{p} \left(\log \frac{D^2 + (2\delta + sp)^2}{\frac{d^2}{4} + (2\delta + sp)^2} + \frac{D^2}{3(D^2 + (2\delta + sp)^2)} \right. \\ & \left. + 4 \frac{2\delta + sp}{D} \text{atan} \frac{D}{2\delta + sp} - 4 \right) dp \end{aligned} \quad (30)$$

Here δ denotes the mesh height over the interface, J_2 is the Bessel function, and parameter

$$s = \frac{1}{jk\sqrt{\epsilon_r - 1}} \quad (31)$$

For the zero distance from the grid to the interface $\delta = 0$ the integral is difficult to calculate numerically, because of a (weak) singularity, but for $\delta \neq 0$ it can be done with no complications. The results show that for the case of moderate contrasts ($\epsilon_r < 3$) the relative correction Δ is very small[‡] at low frequencies ($D \ll \lambda$) and small δ . This follows from (30) for $\delta \rightarrow 0$ explicitly. Since the domain $p \ll 1$ almost does not contribute into the integral due to the presence of the Bessel function, one can consider the value $|sp|$ as a large parameter as compared to D and $d/4$ at low frequencies. Then the expression inside the brackets in (30) tends to zero when $k \rightarrow 0$, which means that $\Delta \rightarrow 0$, too.

The resulting modification of the formula for the equivalent surface impedance (9) and (10) is minor: the value of κ should be replaced by $\kappa(1 - \Delta)$. Also, the effective capacitance (12) can be corrected by multiplying by $(1 - \Delta)$.

4. COMPARISON WITH THE LOCAL QUASI-STATIC MODEL AND EXPERIMENT

Artificial impedance surface with square patches was studied in [1] using numerical techniques. In particular, dispersion curves for surface

[‡] For the example considered in the next section, the correction is about $\Delta = -0.0055 - j0.0006$ and can be neglected.

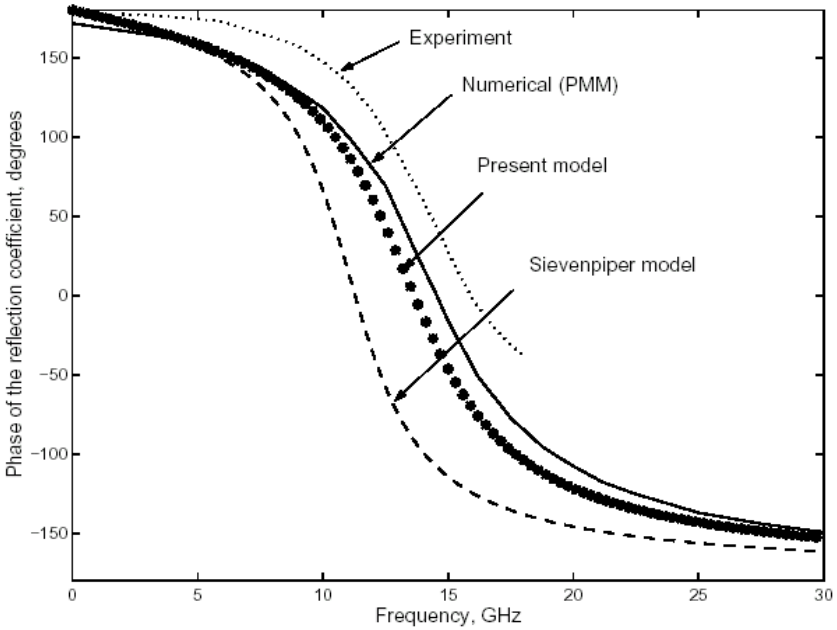


Figure 2. Frequency behavior of the phase of the reflection coefficient. Dotted and solid lines show results of paper [6]. Dashed line has been calculated using the quasi-static formula (16) from [1].

waves along the structure were plotted in Figure 10 of that paper. In that picture, the point at which TE surface wave curve crosses the speed-of-light line corresponds to the resonant frequency of the equivalent surface impedance calculated here.[§] From the numerical model [1] this resonant frequency is approximately 14.4 GHz, the present model gives 14.37 GHz, and the local and quasi-static model [2] gives 11.65 GHz.

More detailed comparison can be made with data for the phase of the reflection coefficient at normal incidence, which are available in the literature [6]. In that work, the reflection coefficient was calculated numerically using the periodical method of moments and measured experimentally. The surface parameters are the following: $D = 2.44$ mm, $d = 0.15$ mm, $\epsilon_r = 2.51$, and $h = 1.57$ mm. We have extracted the numerical and experimental data from the corresponding plots in [6] (Figure 32a, page 67, and Figure 36a, page 81) and plotted them together with the data calculated using the present model. For comparison, the corresponding results of the previous quasi-static

[§] TE surface waves are guided by the impedance surface at higher frequencies.

model are also shown. Obviously, the dynamic model much better matches the numerical and experimental data.

Finally, we would like to observe that the patch shape (rectangular or hexagonal) does not change the result much. We have calculated the reflection phase for the surface with hexagonal patches studied in [1] using the model of rectangular patch array with the same period and the same width of the gaps between patches, and it has been found that the result is quite close to that plotted in Figure 14 of paper [1].

5. CONCLUSION

In this paper, a dynamic model for novel artificial impedance surfaces (dense arrays of small metal patches over conducting surfaces) has been presented. This simple analytical model takes into consideration electromagnetic interactions in the infinite array, the presence of a dielectric layer between patches and the ground, and higher-order Floquet modes inside the structure in the absence of dielectric. Comparison with available experimental and numerical data shows quite good agreement. The model clearly shows the influence of various factors on the properties of the artificial surface and can be used in the design of microwave devices which make use of this new structure. This can help to avoid extensive numerical simulations and analytically optimize composite layers for particular applications in the antenna and waveguide techniques. Possible extensions of the model allow the analysis of resonant arrays.

ACKNOWLEDGMENT

This work was supported by Nokia Research Center, Filtronic LK, and TEKES. Partial support of Prof. Simovski from the Russian Ministry of Education, grant No. TOO 2.4-2127 is gratefully acknowledged.

REFERENCES

1. Sievenpiper, D., L. Zhang, R. F. J. Broas, N. G. Alexopoulos, and E. Yablonovich, "High-impedance electromagnetic surfaces with a forbidden frequency band," *IEEE Trans. Microwave Theory Techniques*, Vol. 47, 2059–2074, 1999.
2. Sievenpiper, D. F., "High-impedance electromagnetic surfaces," Ph.D. Thesis, University of California at Los Angeles, 1999. Available at www.ee.ucla.edu/labs/photon/thesis/ThesisDan.pdf

3. Diaz, R. E., J. T. Aberle, and W. E. McKinzie, "TM mode analysis of a Sievenpiper high-impedance reactive surface," *Antennas and Propagation Society International Symposium*, Vol. 1, 327–330, 2000.
4. Yang, H.-Y. D., R. Kim, and D. R. Jackson, "Design consideration for modeless integrated circuit substrates using planar periodic patches," *IEEE Trans. Microwave Theory Techn.*, Vol. 48, No. 12, 2233–2239, 2000.
5. Sievenpiper, D. F. and E. Yablonovich, "3D metallo-dielectric photonic crystals with strong capacitive coupling between metallic islands," *Phys. Rev. Lett.*, Vol. 80, No. 13, 2829–2832, 1998.
6. Saville, M. A., "Investigation of conformal high-impedance ground planes," Thesis AFIT/GE/ENG/00M-17, Air Force Institute of Technology, Wright-Patterson Air Force Base, Ohio. Available at www.au.af.mil/au/database/research/ay2000/afit/afit-ge-eng-00m-17.htm
7. Yang, F.-R., K.-P. Ma, Y. Qian, and T. Itoh, "A novel TEM waveguide using uniplanar compact photonic-bandgap (UC-PBG) structure," *IEEE Trans. Microwave Theory Techniques*, Vol. 47, 2092–2098, 1999.
8. Tretyakov, S. A. and C. R. Simovski, "Wire antenna near artificial impedance surface," *Microwave and Optics Technology Letters*, Vol. 27, No. 1, 46–50, 2000.
9. Kontorovich, M. I., M. I. Astrakhan, V. P. Akimov, and G. A. Fersman, *Electrodynamics of Grid Structures*, Moscow, Radio i Svyaz, 1987 (in Russian).
10. Yatsenko, V. V., S. A. Tretyakov, S. I. Maslovski, and A. A. Sochava, "Higher order impedance boundary conditions for sparse wire grids," *IEEE Transactions on Antennas and Propagation*, Vol. 48, No. 5, 720–727, 2000.
11. DeLyser, R. R. and E. F. Kuester, "Homogenization analysis of electromagnetic strip gratings," *J. Electromagn. Waves Applic.*, Vol. 5, No. 11, 1217–1236, 1991.
12. Compton, R. C., L. B. Whitbourn, and R. C. McPhedran, "Strip gratings at a dielectric interface and application of Babinet's principle," *Applied Optics*, Vol. 23, No. 18, 3236–3242, 1984.
13. Whitbourn, L. B. and R. C. Compton, "Equivalent-circuit formulas for metal grid reflectors at a dielectric boundary," *Applied Optics*, Vol. 24, No. 2, 217–220, 1985.
14. Sochava, A. A., "Diffraction of electromagnetic waves by a semi-infinite grid positioned at the Earth surface," M.Sc. Thesis,

Leningrad Polytechnic Institute, 1987 (in Russian).

15. Kong, J. A., *Electromagnetic Wave Theory*, J. Wiley & Sons, 1986.
16. Wait, J. R., "Reflection from a wire grid parallel to a conducting plane," *Canadian Journal of Physics*, Vol. 32, 571–579, 1954.
17. Polikarpov, G. I., "Study of electromagnetic wave diffraction by metallic meshes located in layered media," Candidate of Sciences (Ph.D.) Thesis, St. Petersburg State Technical University, 1994 (in Russian).

Sergei A. Tretyakov received the Dipl. Engineer-Physicist, the Ph.D., and the Doctor of Sciences degrees (all in radiophysics) from the St. Petersburg State Technical University (Russia), in 1980, 1987, and 1995, respectively. From 1980 to 2000 he was with the Radiophysics Department of the St. Petersburg State Technical University. Presently, he is professor of radio engineering in the Radio Laboratory, Helsinki University of Technology. His main scientific interests are electromagnetic field theory, complex media electromagnetics, and microwave engineering. Prof. Tretyakov served as Chairman of the St. Petersburg IEEE ED/MTT/AP Chapter from 1995 to 1998.

Constantin R. Simovski received the Dipl. Engineer-Physicist, the Ph.D., and the Doctor of Sciences degrees (all in radiophysics) from the St. Petersburg State Technical University (Russia), in 1980, 1986, and 2000, respectively. From 1980 to 1992 he was with the research and industrial firm "Impulse" (Leningrad, USSR). Since 1992 he has been with the Physics Department of the St. Petersburg State Institute of Fine Mechanics and Optics, St. Petersburg, Russia. Presently, he is professor in this department. His main scientific interests are electromagnetic field theory, complex media electromagnetics, and non-linear optics of wave beams.